Synthesis and Characterization of an Octacationic Iron(III) Tetraphenylporphyrin, Which Is Soluble in Water and Non-μ-Oxo Dimer Forming

Örn Almarsson,† Helgi Adalsteinsson, and Thomas C. Bruice*

Contribution from the Department of Chemistry, University of California at Santa Barbara, Santa Barbara, California 93106

Received May 25, 1994®

Abstract: Synthesis and characterization {electrospray mass spectroscopy, UV/vis spectra, and ^1H and ^{13}C NMR, and purity by gel electrophoresis} of the sterically hindered, polycationic water-soluble iron(III) *meso*-5,10,15,20-tetrakis(2,4,6-trimethyl-3,5-bis{α-*N*,*N*,*N*-trimethylammoniummethyl}phenyl)porphyrin octachloride dihydrate (**3**)-$Fe^{III}(X)_2$ (where X = H_2O and/or HO^-, dependent on pH) is reported. The synthesis of the ligand $\mathbf{3}H_2$ rests on the discovery of a highly selective bromomethylation reaction of *meso*-5,10,15,20-tetrakis(2,4,6-trimethylphenyl)porphyrin (tetramesitylporphyrin, $\mathbf{TMP}H_2$) with formaldehyde and HBr/acetic acid. The electrophoretic mobilities of octacationic $\mathbf{3}H_2$ and (**3**)$Fe^{III}(H_2O)_2$ were comparable, being slightly more than twice the mobilities of the free bases and iron(III) complexes of the commercially available tetracationic porphyrins tetrakis(*N*-methylpyridyl)porphyrin ($\mathbf{TMPyP}H_2$) and tetrakis(4-trimethylammoniumphenyl)porphyrin ($\mathbf{TMAP}H_2$). μ-Oxo dimer formation is not detectable with (**3**)-$Fe^{III}(X)_2$. The determined pK_as of the water ligands of polycationic (**3**)$Fe^{III}(H_2O)_2$ increase with increasing ionic strength, whereas the pK_a values of the previously studied polyanionic tetrakis(2,6-dimethyl-3-sulfonatophenyl)-porphyrin iron(III) {(**1**)$Fe^{III}(H_2O)_2$} decrease with increasing ionic strength. This is consistent with an increase in the electropositive nature of the iron center of (**3**)$Fe^{III}(H_2O)_2$. A marked tendency of cationic (**3**)$Fe^{III}(X)_2$ to ligate buffer anions was observed. This feature is not shared by the polyanionic (**1**)$Fe^{III}(X)_2$. Spectrophotometric titrations of (**3**)$Fe^{III}(H_2O)_2$ with acetate buffer and fitting of absorbance changes at 398 nm vs $[HOAc]_t$ afforded a pH-independent binding constant K_B of 42 M^{-1} for monoligation of acetate.

Introduction

Reactions of peroxidase and monooxygenase enzymes employing iron−porphyrin cofactors is of continuing biological and chemical interest. Catalase[1] and peroxidases[2] react with peroxides in what are formally two-electron redox reactions. Reaction of hydrogen peroxide with the iron(III) porphyrin cofactor converts the latter to an iron(IV)−oxo porphyrin π-cation radical, compound I, which is two oxidation equivalents above the resting enzyme. Compound I is therefore the product of a net heterolytic cleavage of H_2O_2. Hydroperoxides can replace the usual $1e^- + O_2 + 1e^-$ oxidant of the protoporphyrin-IX of cytochrome P-450. The intermediate produced by this so-called "peroxide shunt" (Scheme 1) has been assumed to be a compound I species, based upon the nature of substrate oxidation products obtained by use of the shunt mechanism.[3,4] It is not clear, however, if the rate controlling step in the catalase, peroxidase, and cytochrome P-450 shunt mechanisms is O−O bond heterolysis (eq 1) or a homolysis (eq 2).

$$\{(\text{porphyrin})Fe^{III}\}^+ + ROOH \rightarrow \{(\text{porphyrin}^{\bullet+})Fe^{IV}{=}O\}^+ + ROH \quad (1)$$

$$\{(\text{porph})Fe^{III}\}^+ + ROOH \xrightarrow{\text{r.d.s.}} \{(\text{porph})Fe^{IV}OH,RO^{\bullet}\}^+ \xrightarrow{\text{fast}} \{(\text{porph}^{\bullet+})Fe^{IV}{=}O\}^+ + ROH \quad (2)$$

In model studies from this laboratory[5−7] involving reactions of water-soluble iron(III) tetraphenylporphyrin derivatives with a variety of hydroperoxides, we have shown that the rate-limiting step involves homolytic cleavage of the O−O bonds of alkyl ROOH, although heterolysis is the pathway with acyl peroxides and those alkyl hydroperoxides where RO^- is a good leaving group.[7a,d] Studies of the mechanism of O−O bond cleavage of hydroperoxides on reaction with iron(III) porphyrins in water are continued in the following paper in this issue.

In previous studies in water we have employed as catalysts tetrakis(2,6-dimethyl-3-sulfonatophenyl)porphinatoiron(III)[7e] and tetrakis(2,6-dichloro-3-sulfonatophenyl)porphinatoiron(III) dihydrates {(**1**)$Fe^{III}(X)_2$ and (**2**)$Fe^{III}(X)_2$, respectively, where X = H_2O or HO^-; Chart 1} as catalysts for the decomposition of

† In partial fulfillment of the Ph.D. degree in chemistry.

® Abstract published in *Advance ACS Abstracts*, March 15, 1995.

(1) Schonbaum, G. R.; Chance, B. In *The Enzymes*, 2nd ed.; Boyer, P. D., Ed.; Academic Press: New York, 1976; Vol. 13, pp 363−408.

(2) *Peroxidases in Chemistry and Biology*; Everse, J., Everse, K. E., Grisham, M. B., Eds.; CRC Press: Boca Raton, FL, 1991; Vol. 2.

(3) *Cytochrome P-450; Structure, Mechanism and Biochemistry*; Ortiz de Montellano, P. R., Ed.; Plenum: New York, 1986.

(4) (a) Dolphin, D.; Forman, A.; Borg, D. C.; Fajer, J.; Felton, R. H. *Proc. Natl. Acad. Sci U.S.A.* **1971**, *68*, 614. (b) Moss, T. H.; Ehrenberg, A.; Beardon, A. J. *Biochemistry* **1969**, *8*, 4159. (c) Schulz, C. E.; Devaney, P. W.; Winkler, H.; Debrunner, P. G.; Doan, N.; Chiang, R.; Rutter, R.; Hager, L. P. *FEBS Lett.* **1979**, *103*, 102. (d) Roberts, J. E.; Hoffman, B. M.; Rutter, R.; Hager, L. P. *J. Biol. Chem.* **1981**, *256*, 2118. (e) Marnett, L. J.; Weller, P.; Battista, J. R. In Cytochrome P-450-Structure, Mechanism and Biochemistry; Ortiz de Montellano, P. R., Ed.; Plenum Press: New York, 1986; Chapter 2.

(5) Bruice, T. C. In *Mechanistic Principles of Enzymatic Activity*; Liebman, J. F., Greenberg, A., Eds.; VCH Publishers, Inc.: Deerfield Beach, FL, 1988; Chapter 6, pp 227−277.

(6) For reviews on the reactions of water soluble metallotetraphenylporphyrins with hydroperoxides, see: (a) Bruice, T. C. *Acc. Chem. Res.* **1991**, *24*, 243−249. (b) Bruice, T. C. *Aldrich Chim. Acta* **1988**, *21*, 87.

(7) (a) Bruice, T. C.; Balasubramanian, P.; Lee, R. W.; Lindsey Smith, J. R. *J. Am. Chem. Soc.* **1988**, *110*, 7890. (b) Lindsay Smith, J. R.; Balasubramanian, P. N.; Bruice, T. C. *J. Am. Chem. Soc.* **1988**, *110*, 7411. (c) Gopinath, E.; Bruice, T. C. *J. Am. Chem. Soc.* **1991**, *113*, 4657. (d) Balasubramanian, P.; Lee, R. W.; Bruice, T. C. *J. Am. Chem. Soc.* **1989**, *111*, 8714. (e) Zipplies, M. F.; Lee, W. A.; Bruice, T. C. *J. Am. Chem. Soc.* **1986**, *108*, 4433.

0002-7863/95/1517-4524$09.00/0

Scheme 1

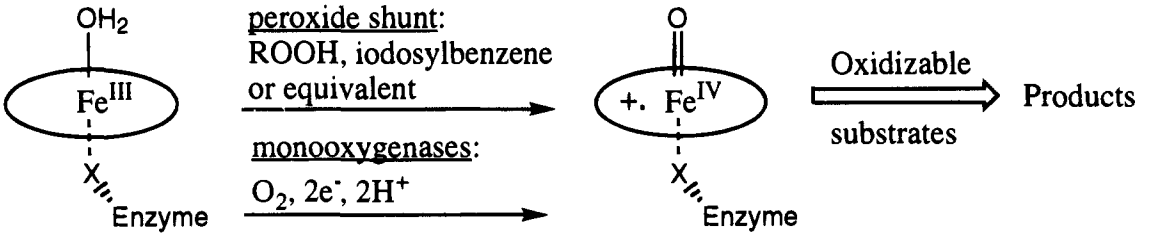

Chart 1

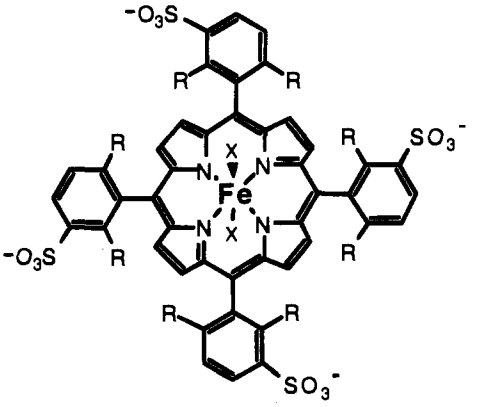

(**1**)$Fe^{III}(X)_2\{Na^+\}_4$ R = CH_3

(**2**)$Fe^{III}(X)_2\{Na^+\}_4$ R = Cl

(X = H_2O/HO^-)

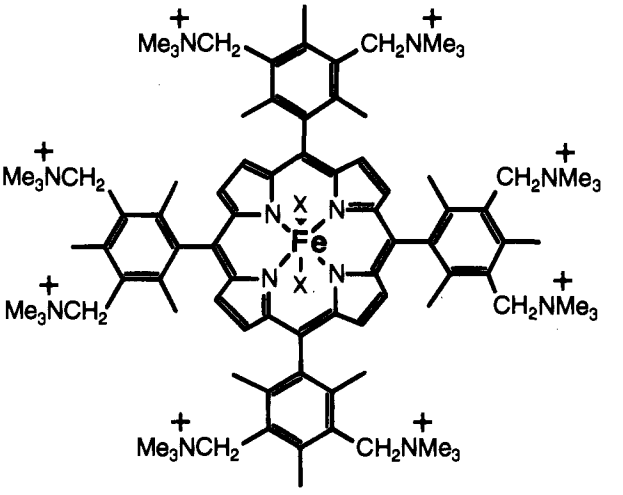

(**3**)$Fe^{III}(X)_2$ $\{Cl^-\}_8$

Chart 2

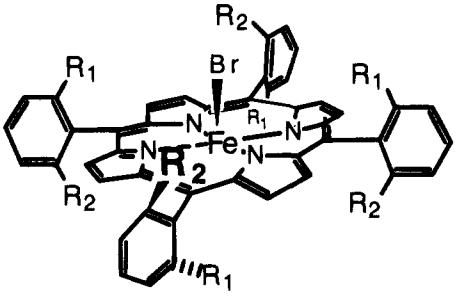

(αβαβ-**TMNP**)$Fe^{III}Br_5$

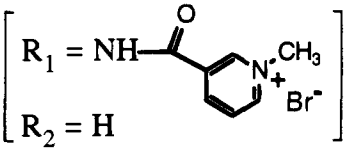

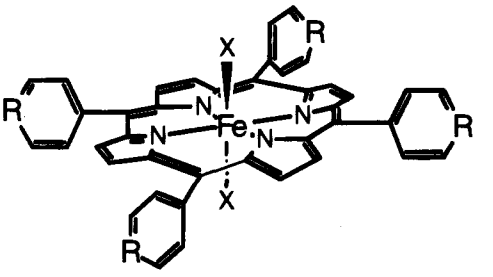

(**TMPyP**)$Fe^{III}(X)_2$ R = NCH_3^+

(**TMAP**)$Fe^{III}(X)_2$ R = C-$N(CH_3)_3^+$

t-BuOOH, as well as other alkyl and acyl hydroperoxides. A question is whether the four anionic charges of the porphyrin rings of (**1**)$Fe^{III}(X)_2$ and (**2**)$Fe^{III}(X)_2$ have some influence upon the rate and equilibrium constants and possibly the identity of products from reactions of these species with hydroperoxides. Cationic functional groups in enzyme active sites have been suggested to influence the nature of the O–O bond breaking step. Poulos and Kraut postulated that the conserved arginine 48, located in close proximity of the axial water ligand to iron in the X-ray structure of cytochrome *c* peroxidase, electrostatically assists a heterolytic scission of hydrogen peroxide {by stabilizing the HO^- leaving group} when the latter becomes the axial ligand.[8] One might note that no positively charged substituent residue resides at the active site of cytochrome P-450_{CAM} camphor hydroxylase from *P. putida*.[9]

Aggregation and μ-oxo dimer formation has limited the utility of the commercially available tetracationic porphyrins, which include (Chart 2) *meso*-5,10,15,20-tetrakis(4-trimethylammoniumphenyl)porphinatoiron(III) chloride {(**TMAP**)Fe^{III}(Cl)} and *meso*-5,10,15,20-tetrakis(*N*-methylpyridyl)porphinatoiron(III) chloride {(**TMPyP**)Fe^{III}(Cl)} in aqueous solution.[10,11] So far, only one cationic tetraphenylporphyrin ligand has been found to be effective in preventing μ-oxo dimerization of its iron(III) complex in aqueous solution at intermediate to high pH. The compound, *meso*-αβαβ-tetrakis(*o*-(*N*-methylnicotinamido)phen-

(8) Poulos, T. L.; Kraut, J. *J. Biol. Chem.* **1980**, *255*, 8199.

(9) Poulos, T. L.; Finzel, B. C.; Howard, A. J. *J. Mol. Biol.* **1987**, *195*, 687.

(10) One precedent exists for solution kinetics of (**TMPyP**)$Fe^{III}(X)_2$ with *tert*-butyl hydroperoxide in water. See: Lindsay Smith, J. R.; Lower, R. J. *J. Chem. Soc., Perkin Trans 2* **1991**, 31.

yl)porphyrinatoiron(III) bromide, {($\alpha\beta\alpha\beta$-**TMNP**)Fe^{III}(Br), Chart 2}, was shown by Miskelly, Webley, Clark, and Buckingham[12] to exist as a monomer over a wide range of concentrations and pH.[13] In our judgment, excessive crowding at the iron site renders this compound less desirable for comparisons with the anionic porphyrins (**1**)$Fe^{III}(X)_2$ and (**2**)$Fe^{III}(X)_2$.

Our interest in the present study is to develop a porphyrin ligand which is (i) water-soluble, (ii) polycationic, (iii) easily synthesized, and (iv) sufficiently crowded on the faces of the porphyrin to deter unwanted μ-oxo dimer formation. We report the synthesis and characterization of octacationic *meso*-5,10,-15,20-tetrakis(2,4,6-trimethyl-3,5-bis{α-*N,N,N*-trimethylammoniummethyl}phenyl)porphyrin octachloride (**3**H_2) and its iron-(III) complex (**3**)$Fe^{III}(X)_2$ (Chart 1). The electronic effects of the peripheral quaternary ammonium ions on the acid dissociation constants of the axial ligated water in (**3**)$Fe^{III}(X)_2$ (where X = H_2O and HO^-), were studied by spectrophotometric pH titrations and compared to the like constants for (**1**)$Fe^{III}(X)_2$.

Experimental Section

Materials. Formaldehyde (polymeric solid), mesitaldehyde, pyrrole, BF_3–etherate, 30% HBr in glacial acetic acid, and gaseous trimethylamine (99%) were purchased from Aldrich and used as received. Tetramesitylporphyrin (**TMP**H_2) was synthesized by the method of Lindsey and Wagner, in commercial grade chloroform (Fisher).[14] Glacial acetic acid, methylene chloride, and hexane were obtained from Fisher. Tetracationic porphyrins (**TMAP**)Fe^{III}Cl and **TMAP**H_2 were purchased from Midcentury, while **TMPyP**H_2 was obtained from Strem Chemicals Inc. (**TMPyP**)Fe^{III}Cl was prepared from **TMPyP** by the method of Adler.[15] Preparative thin-layer chromatography plates (20 × 20 × 0.025 and 20 × 20 × 0.05 cm) were purchased from E. Merck.

Instrumentation. ^{1}H and proton decoupled ^{13}C NMR spectra were recorded on a General Electric GN-500 spectrometer operating at 500 (^{1}H) and 125 MHz (^{13}C), at 25 °C. Standard parameters were employed, except when paramagnetic iron(III) porphyrin samples were studied, where the following adjustments were made: Acquisition delay of 5 ms, spectral width of 80 000 Hz, and typical number of scans of around 50 000 were used on 3 mM iron porphyrin samples in 5 mm tubes. Electrospray and fast-atom bombardment mass spectra were recorded at UCLA by Dr. Kym Faul and at UC Berkeley by Dr. Than Dang. UV–visible absorption spectra were obtained on a CARY-14 spectrometer, interfaced with a Gateway 2000 PC computer running On-Line Instruments (OLIS, Bogart, GA) software. Gel electrophoresis was performed on a HBI vertical slab gel system with a FB 650 power supply (Fisher Biotech). Typically, 80–100 V were applied across 17.8 cm long gel slabs (2 × 120 mm) at 300 mA current. The gels were composed of either 16–24% polyacrylamide (5% total crosslinking) or Hydrolink D-600 (AT Biochem) at 7–10% density. The buffer consisted of 0.1 M K_2HPO_4 and 0.05 M citric acid.[16] The cationic porphyrins were allowed to migrate toward the cathode by switching the leads in the inputs of the power supply. Radiometer model 26 pH-meter and Fisher 13-620-280 microglass electrode were used for proton activity measurements. No sodium ion correction is necessary up to pH 12.5. A 3 M $NaNO_3$ solution for adjustment of ionic strength was prepared from reagent grade material and passed through a Chelex column prior to use. Spectrophotometric pK_a determinations were conducted on a computer interfaced CARY-15 spectrophotometer (UCSB Chemistry Electronics shop) in a large volume thermostated cell (30 °C, pathlength 3.387 cm)[17] at starting volumes of 25.0 mL. Titrations were performed with incremental recording of absorption spectra from 700 to 360 nm. Final volumes were typically 25.5 mL (2% increase). pH was constantly measured with the Fisher glass electrode with constant magnetic stirring of the cell contents. Titration of iron(III) porphyrin (~5 × 10^{-7} M) in water by addition of aliquots of 4.4 M acetate buffer was carried out on the CARY-15 spectrophotometer in the large volume cell at 30 °C.

Table 1. Intermediates and Products from Bromomethylation Reactions of **TMP**H_2

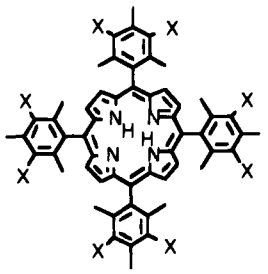

intermediate	X = CH_2Br	X = H	no. of isomers
5a	1	7	1
5b	2	6	5
5c	3	5	5
5d	4	4	10
5e	5	3	5
5f	6	2	5
5g	7	1	1
4	8	0	1

Synthesis. 5,10,15,20-Tetrakis(2,4,6-trimethyl-3,5-bis{α-bromomethyl}phenyl)porphyrin (4) was prepared using the bromomethylating system of Van der Made.[18] **TMP**H_2 (48 mg, 0.063 mmol), formaldehyde (300 mg, 10 mmol), and glacial acetic acid (10 mL) were placed in a predried 10-mL round-bottom flask fitted with a reflux condenser. The stirred suspension was treated with HBr/acetic acid solution (5 mL, 10 mmol) which resulted in dissolution and a color change to deep green. The flask was immersed in a heating bath at 105 °C and stirred well in the dark. After 72 h the reaction was cooled and extracted with chloroform against added water. The chloroform extracts were combined and shaken with 5% sodium bicarbonate, water, and brine. The chloroform was then dried over Na_2SO_4 and filtered quickly through a plug of silica gel. The brown solution was evaporated, and the residue, containing mainly **4** and **5g** (see Table 1 for all isolable intermediates of this reaction) was subjected to chromatography on silica gel. **4** has an R_f of 0.33 (Merck Kieselgel 0.25 mm thickness) in 1:1 chloroform/hexane. Preparative TLC was performed on at least two plates in this solvent in a darkened chamber. Elution was followed by rapid air drying, scraping, and elution of the porphyrin from the gel with methylene chloride (~40 mL). Evaporation of solvent afforded 29 mg (30%) of **4**: mp > 230 °C, UV/vis spectrum λ_{max} (log ϵ) 402 (sh), 420 (5.6), 519 (4.5), 547 (4.3), 590 (4.3), 648 (4.2); ^{1}H NMR ($CDCl_3$, 500 MHz) δ (ppm) 8.53 (s, 8H, β-pyrrole C-H), 4.82 (s, 16H, CH_2Br), 2.79 (s, 12H, *p*-CH_3Ph), 1.92 (s, 24H, *o*-CH_3-Ph), −2.42 (br s, 2H, pyrrole N-H); ^{13}C NMR ($CDCl_3$, 125 MHz) δ (ppm) 140.36, 140.19, 139.98, 137.60, 129.34, 118.25, 116.13, 112.31 (aromatic C), 15.49 (*p*-CH_3Ph), 18.89 (*o*-CH_3Ph); MS (FAB, nitrobenzyl alcohol matrix) calcd for $C_{52}H_{38}N_4Br_8$ [M^+] (*m/z*) 1525.8 (center of a broad cluster of 14 peaks due to various combinations of isotopes), found 1525.1 (M^+ center of a broad peak).

Synthesis of 5,10,15,20-Tetrakis(2,4,6-trimethyl-3,5-bis{α-*N,N,N*-trimethylammoniummethyl}phenyl)porphyrin Octachloride (3H_2). A freshly prepared sample of **4** (5.0 mg, 3.3 μmol) was dissolved in dry DMF (2 mL) and transferred to a two-necked, round-bottom flask, containing a magnetic stirbar. Trimethylamine was bubbled into the solution at 2 °C periodically over 1 h and, in between, the solution was gently stirred. The solution was allowed to warm to room temperature with stirring. Water (5 mL) was added, followed by chloroform (5 mL). The biphase was transferred to a small separatory funnel, shaken, and allowed to separate. The chloroform layer was removed, and the remaining deep red aqueous layer was shaken again with chloroform (5 mL). After separation of the layers, the aqueous

(11) For other recently reported cationic porphyrins: (a) Lavallee, D. K.; Xu, D.; Pina, R. *J. Org. Chem.* **1993**, *58*, 6000. (b) Pethö, G.; Elliott, N. B.; Kim, M. S.; Lin, M.; Dixon, D. W.; Marzilli, L. G. *J. Chem. Soc., Chem. Commun.* **1993**, 1533. (c) Pandey, R. K.; Shiau, F.-Y.; Smith, N. W.; Dougherty, T. J.; Smith, K. M. *Tetrahedron* **1992**, *48*, 7591. (d) Kuroda, Y.; Hatakeyama, H.; Inakoshi, N.; Ogoshi, H. *Tetrahedron Lett.* **1993**, *34*, 8285.

(12) Miskelly, G. M.; Webley, W. S.; Clark, C. S.; Buckingham, D. A. *Inorg. Chem.* **1988**, *27*, 3773.

(13) A tetracationic porphyrin, (2-TMPyP)Fe^{III}, resists dimerization in three out of four atropisomers, which amount to 87.5% of a statistical mixture at equilibrium. Rodgers, K. R.; Reed, R. A.; Su, Y. O.; Spiro, T. G. *Inorg. Chem.* **1992**, *31*, 2688.

(14) Lindsey, J. S.; Wagner; R. W. *J. Org. Chem.* **1989**, *54*, 828.

(15) Adler, A. D.; Longo, F. R.; Kampas, F.; Kim, J. *J. Inorg. Nucl. Chem.* **1970**, *32*, 2443.

(16) Deyl, Z. In *Electrophoresis—A Survey of Techniques and Applications, part B*; Deyl, Z., Ed.; Elsevier: Amsterdam, 1983; p 45.

(17) See: Bruice, T. C.; Maley, J. R. *Anal. Biochem.* **1979**, *34*, 275.

(18) Van Der Made, A. W.; Van der Made, R. H. *J. Org. Chem.* **1993**, *58*, 1262.

phase was evaporated to dryness. The brownish residue was dissolved in a small amount of water (~0.5 mL) and applied to an anion exchange column (poured and preequilibrated with doubly distilled water) containing Biorad AG1-X8 resin, 200–400 mesh, chloride form. The column was eluted with doubly distilled water, and the fast red band was collected and evaporated to give 5.4 mg (96%) of $3H_2$-octachloride: mp > 230 °C, UV/vis λ_{max} (log ϵ) 397 (sh), 417 (5.5), 518 (4.2), 550 (3.8), 582 (3.9), 635 (3.7); ^{1}H NMR (D_2O) δ (ppm) 8.7 (br s, 8H, β-pyrrole C-*H*), 5.1 (m, 16H, $-CH_2NMe_3$), 3.27 (br s, 72H, $-N[CH_3]_3$), 2.94 (br s, 12H, *p*-CH_3Ph), 1.98 (br s, 24H, *o*-CH_3Ph); ^{1}H NMR (DMSO-d_6) δ (ppm) −2.5 (br s, 2H, pyrrole N-*H*); ^{13}C NMR (D_2O, 125 MHz) δ (ppm) 164.8, 145.2, 141.8, 141.6, 126.0 (aromatic C), 111.4 (*meso*-C), 63.8 ($^{13}CH_2NMe_3$), 53.1 ($-N[CH_3]_3$), 36.8 (*p*-CH_3-Ph), 21.5 (*o*-CH_3Ph); MS (FAB, NBA matrix) 204.9, calcd for $[C_{88}H_{13}N_{12}Cl_8]^{8+}$ 204.8, additional peaks for M/7, M/6, and M/5 are also identified; MS (electrospray, 50% CH_3CN in water with 2 mM NH_4OAc) 241.4 (base peak) calcd for $(M - 5Cl^- + H^+)^{6+}$ 244.1, peaks for $(M - 4Cl^- + H^+)^{5+}$, $(M - 3Cl^- + H^+)^{4+}$, and $(M - 2Cl^- + H^+)^{3+}$ were also observed with a similar distribution of isotope peaks; gel electrophoresis {7% Hydrolink D-600 vertical slab, 24–30 °C, 100 V over 17.8 cm, 5 h}: 7.5 cm migration toward the cathode, ratio of M_{3H_2}/M_{TMAPH_2} is 2.5, ratio of M_{3H_2}/M_{TMPyPH_2} is 1.7 (see Figure 2 and results section for definition and interpretation).

Synthesis of 5,10,15,20-Tetrakis(2,4,6-trimethyl-3,5-bis{α-*N,N,N*-trimethylammoniummethyl}phenyl)porphinatoiron(III) Octachloride Dihydrate {(3)$Fe^{III}(H_2O)_2$}. To a solution of $3H_2$ (11 mg, 6.7 μmol) in distilled water (4 mL) was added anhydrous ferrous chloride (240 mg, 1.9 mmol), and the resulting suspension was heated to reflux for 10 h. After allowing the reddish-brown mixture to cool to room temperature, it was filtered through a cotton plug, and the filtrate evaporated to dryness. The residue was triturated with 0.3 mL distilled water, supernatant was applied to a Sephadex G-10 desalting column, and the column eluted with deionized water. The fast brownish band was collected, and the fractions most concentrated in iron porphyrin (UV–vis assay) were combined. The resulting porphyrin solution was evaporated to near dryness, and the concentrated eluate was applied to a column of Biorad AG1-X8 resin (200–400 mesh, chloride form). After elution with doubly distilled water, the fast porphyrin fractions were combined, diluted to 200 mL with deionized water, and placed in a Amicon 8400 ultrafiltration cell (capacity 250 mL), fitted with an Amicon YC05 membrane filter (molecular weight cutoff ~ 500). The filter had been previously washed with 200 mL 5% NaCl solution, followed by rinsing with 2 × 200 mL deionized water. Concentration was achieved by pressurizing the cell with nitrogen to 55 psi with stirring. The clear filtrate was found to be free or porphyrin by UV–vis spectra. When the volume of the filtrate reached ~20 mL, the contents of the cell were rediluted and concentrated again. This procedure was repeated a second time, such that any free metal impurity in the original sample becomes ~1% of its initial concentration. The final concentrate was evaporated to dryness on a rotary evaporator to give 11 mg (94%) of (3)$Fe^{III}(H_2O)_2$: mp > 230 °C; UV/vis spectra λ_{max} in nm (log ϵ) {H_2O pH 2.1, HCl} 395 (5.11), 416 (5.05), 531 (4.66); {H_2O pH 7.30, 5 mM phosphate buffer} 416 (5.16); {H_2O pH 11.4, NaOH} 417 (5.15); ^{1}H NMR (500 MHz) (D_2O with added DCl, pD ~ 2) δ 55 (ω ~ 1200 Hz), (D_2O at ambient pD) δ 81 (ω ~ 1000 Hz), (D_2O with added NaOD, pD ~ 12) δ 82 (ω~500 Hz); MS (electrospray, 50% CH_3CN in water with 2 mM NH_4OAc) calcd for $C_{88}H_{132}N_{12}Cl_8Fe$, 1692, found ($M^+$); gel electrophoresis {7% Hydrolink D-600 vertical slab, 24–30 °C, 80 V over 17.8 cm, 5 h}: 7.0 cm migration toward the cathode, the mobility ratio M_{3Fe}/M_{TMAPFe} is 3.9. $M_{3Fe}/M_{TMPyPFe}$ is 2.9.

Results

Synthesis of the octacationic porphyrin ligand $3H_2$ and iron complex (3)$Fe^{III}(X)_2$ is shown in Scheme 2. Water-soluble $3H_2$ is derived from the readily available tetramesitylporphyrin ($TMPH_2$) by stepwise direct bromomethylation, using the reagent system of van der Made,[18] followed by displacement of the bromides from the octabromomethylated intermediate **4** by trimethylamine (Scheme 2).

Silica gel TLC product analysis at intervals during the bromomethylation reaction revealed the presence of intermediates (Table 1) of increasing polarity compared with $TMPH_2$ (indicated by decreasing R_f values on silica gel plates with 1:2

Scheme 2

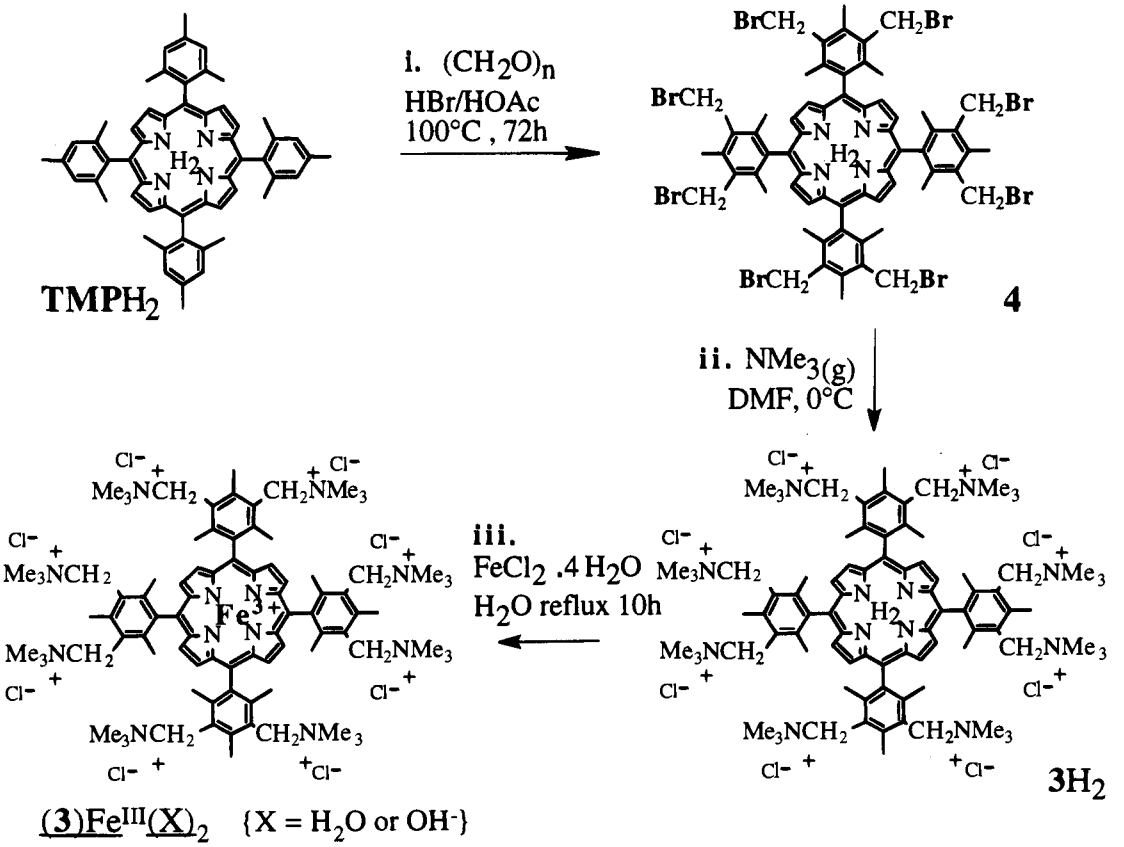

chloroform/hexane eluent). The identities of a number of the bromomethylated intermediates in Table 1 were determined by FAB-mass spectroscopy and proton NMR. The final product, **4**, has an R_f of 0.33 in 1:1 chloroform/hexane and could be purified by plate chromatography (E. Merck silica plates 20 × 20 × 0.025 cm). The heptabromomethylated intermediate **5g**, also present in the final crude mixture, elutes with an R_f of 0.38 under the same conditions. The ^{1}H NMR spectra of penta-, hepta-, and octabromomethylated **TMPH$_2$** derivatives (**5e−g** and **4**), though complicated by the number of possible isomers (Table 1), showed resonances and corresponding integrals in the aromatic region indicative of exclusive reaction of the trimethylphenyl rings and complete retention of the β-pyrrole protons. Thus, the ^{1}H NMR of **4** only shows one β-pyrrole resonance at 8.53 ppm (singlet accounting for 8 H) and a singlet at 4.82 ppm (16 H, assigned to $-CH_2Br$ groups). On the other hand, **5g** displays a pair of closely spaced β-pyrrole doublet resonances centered at 8.5 ppm (8 H), as well as a single resonance at 7.3 ppm, integrating to one proton. Fast-atom bombardment (FAB) mass spectra revealed broad peaks for the molecular ions of **4** and **5g**, due to the isotopic abundances of ^{79}Br and ^{81}Br. A simulated spectrum of **4** (M^+) has 14 peaks spaced between *m/z* 1519.8 and 1532.8. Indeed, the mass spectrum gives a broad peak for the molecular ion, centered at 1525.1 (the calculated *m/z* for M^+ for the most abundant peak is 1525.8 in the simulation). Repeated treatment of mixtures of **4** and **5g** with large excesses of bromomethylating agent in hot acetic acid did not result in enhancement in the yield of **4**.

The octakis(benzylic bromide) **4** is slightly unstable, as evidenced by two-dimensional TLC analysis. All solutions and solid preparations of **4** were stored in the dark under argon. Nucleophilic displacement of the −Br substituents of **4** by various agents provides stable compounds. Pertinent to the present study is the reaction with trimethylamine to give the octacationic porphyrin **3H$_2$**. The reaction was performed with addition of excess gaseous NMe_3 into a solution of **4** in dry DMF in an ice bath. Anion exchange chromatography was used to isolate the product, which was characterized by ^{1}H and ^{13}C NMR, mass spectroscopy, UV−visible absorption spectrum, and gel electrophoresis (*vide infra*). The iron(III) complex was easily obtained by heating of **3H$_2$** with excess ferrous chloride in water. Isolation and purification was performed by gel filtration on Sephadex G-10, anion exchange chromatography, and membrane ultrafiltration to rid the porphyrin of trace metal salts. The brownish solid was characterized by ^{1}H NMR, mass spectroscopy, UV−visible absorption spectra, and gel electrophoresis (*vide infra*). None of the above methods indicated ferric ion nor free base porphyrin contaminant of (**3**)Fe^{III}(X)$_2$. In contrast to **3H$_2$**, the absorption spectrum of (**3**)Fe^{III}(X)$_2$ in water above pH 2 is highly pH-dependent. This is readily understood in terms of the proton dissociation from the two axial water ligands.

A computer generated structure of (**3**)Fe^{III}(H$_2$O)$_2$ is presented in Figure 1. In the idealized model, the iron(III) is placed in the center of the porphyrin plane. The oxygen atoms of the two ligated water molecules located on each side of the porphyrin plane are 8.4 Å away from the nearest four cationic nitrogens in the meta positions. By comparison, the average distance between the oxygen atoms of water ligand and *m*-SO_3^- in a molecular model of (**1**)Fe^{III}(H$_2$O)$_2$ is at least 7.3 Å. When a molecule of H_2O_2 is placed as a ligand to the iron in the model of Figure 1, the terminal unligated oxygen atom of the peroxide is minimally ~8 Å away from a quaternary nitrogen of (**3**)-Fe^{III}(H$_2$O)$_2$.

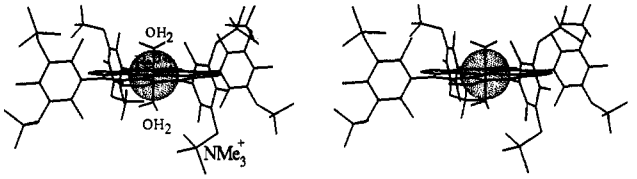

Figure 1. Molecular model of (**3**)Fe^{III}(H$_2$O)$_2$. Hydrogen atoms, except those on the water molecules ligated to the iron(III), are omitted for clarity. The model was built in Quanta 3.3 (MSI, Waltham, MA, 1993) and plotted using the artist plotting routine.

Table 2. Mobility Ratios[a] of Cationic Porphyrins[b] on 7% Hydrolink D-600 Gel[c]

	B		
A	(**3**)Fe^{III}(X)$_2$	(**TMAP**)-Fe^{III}(X)$_2$	(**TMPyP**)-Fe^{III}(X)$_2$
3H$_2$	1.1		
TMAPH$_2$		1.7	
TMPyPH$_2$			1.9
(**3**)Fe^{III}(X)$_2$	1	3.9	2.9
(**TMAP**)Fe^{III}(X)$_2$	0.26	1	0.75
(**TMPyP**)Fe^{III}(X)$_2$	0.34	1.3	1

[a] M_A/M_B are unitless ratios of migration distances for porphyrins A and B, measured from the gel. [b] See Charts 1 and 2 for structures. [c] Gel electrophoresis conditions and materials are described in the Experimental Section.

Gel Electrophoresis of Cationic Porphyrins. As a possible analytical tool and a measure of purity, we investigated the use of gel electrophoresis on the newly synthesized **3H$_2$** and (**3**)-Fe^{III}(X)$_2$. The electrophoretic behavior was compared with that of two well-known tetracationic porphyrins, tetrakis(*N*-methylpyridyl)porphyrin (**TMPyPH$_2$**) and tetrakis(4-trimethylammoniumphenyl)porphyrin (**TMAPH$_2$**) as well as their corresponding iron(III) complexes (Chart 2). Separations were performed on high density polyacrylamide gels (16−24% with 5% of the total percentage as cross-links) as well as on hydrolink D-600 gels (7-10%), under conditions where the compounds were allowed to migrate toward the cathode. The monomeric tetracationic porphyrins and their iron(III) monomeric complexes **TMPyPH$_2$**, (**TMPyP**)Fe^{III}(X)$_2$, **TMAPH$_2$**, and (**TMAP**)Fe^{III}-(X)$_2$ were all found to have very similar electrophoretic mobilities on polyacrylamide gels. The mobilities of **3H$_2$** and (**3**)Fe^{III}(X)$_2$ in that medium were roughly double those of the tetracationic ligands and complexes, as would be expected for a doubling of the formal charge. In contrast to polyacrylamide gels, hydrolink D-600[19] showed separation of free base porphyrins and their corresponding iron(III) complexes. This feature allows assessment of purities as well as suggesting the possibility of separating water soluble metallo- and free base porphyrin mixtures by the use of slab gel electrophoresis. The results of electrophoresis on a 7% hydrolink D-600 gel are shown in Figure 2. Mobility ratios for a standard **B** and pertinent analyte **A** $\{M_A/M_B\}$ measured from the gel of Figure 2 are listed in Table 2. M_A/M_B are more informative than absolute distances of migration on a gel, since the former are independent of voltage, current, power, and the length of time current is applied. Greater mobilities of free base porphyrins are observed when compared with the corresponding iron complexes (Figure 2). Thus, when **A** = (porphyrin)H$_2$ and **B** = (porphyrin)Fe^{III} the values of M_A/M_B range from 1.1 to 1.9 (Table 2). In addition to the expected bands for (**TMPyP**)-Fe^{III}(X)$_2$ and (**TMAP**)Fe^{III}(X)$_2$, there was observed a large amount of the μ-oxo dimer {(**TMPyP**)Fe^{III}}$_2$O and detectable amounts of {(**TMAP**)Fe^{III}}$_2$O (Figure 2). The assignment of the faster moving bands as μ-oxo dimers is based on the observed increase in electrophoretic mobility of the complexes

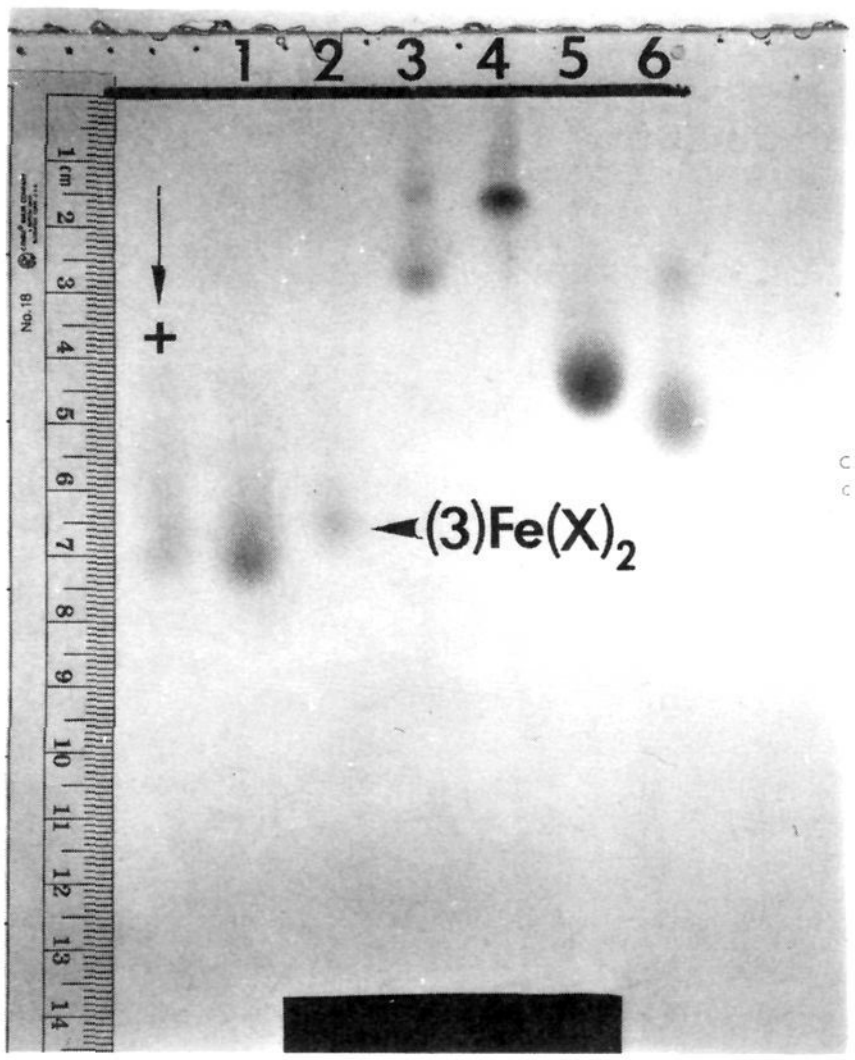

Figure 2. Electrophoresis of cationic water soluble porphyrins on hydrolink D-600 (AT Biochem) 7% vertical slab gel: lane 1, $\mathbf{3}H_2$; lane 2, $(\mathbf{3})Fe^{III}(X)_2$; lane 3, $\mathbf{TMAP}H_2$; lane 4, $(\mathbf{TMAP})Fe^{III}(X)_2$; lane 5, $\mathbf{TMPyP}H_2$; lane 6, $(\mathbf{TMPyP})Fe^{III}(X)_2$ (see Charts 1 and 2 for structures).

relative to the monomers as well as the known propensity of cationic iron porphyrins to undergo μ-oxo dimerization at intermediate and high pH.[12] The mobilities of the bands for octacationic complexes $\{(\mathbf{TMPyP})Fe^{III}\}_2O$ and $\{(\mathbf{TMAP})Fe^{III}\}_2O$ approach the mobility of the octacationic porphyrin $\mathbf{3}H_2$. The increased molecular size of the dimers presumably somewhat retards their migration in the gel, relative to the monomer $\mathbf{3}H_2$ and $(\mathbf{3})Fe^{III}(X)_2$ of similar total charge. No dimerization of $(\mathbf{3})Fe^{III}(X)_2$ was observed, and the compound was shown to be pure by this method.

Determinations of pK_a Values for $(\mathbf{3})Fe^{III}(H_2O)_2$ by Spectrophotometric Titration. The visibile absorption spectrum of $(\mathbf{3})Fe^{III}(X)_2$ changes markedly as a function of pH, due to changes in the identities of the axial ligands X (H_2O and/or HO^-) in aqueous solution. Figure 3 shows visible absorption spectra at various pH values, at a constant ionic strength (μ) of 0.20 (maintained with $NaNO_3$). A plot of absorbance changes at 398 and 417 nm vs pH is shown in Figure 4. The points are experimental, and the fits of the dotted lines to the points have been generated from an equation for dissociations of a diprotic acid (eq 3), as is the case of eqs 4a and 4b. In eq 3, a_H represents proton activity, ϵ are extinction coefficients for the

$$\text{absorbance} = \left\{\frac{a_H{}^3\epsilon_{pH2} + a_H\epsilon_{pH}K_{a1} + \epsilon_pK_{a1}K_{a2}}{a_H{}^2 + a_HK_{a1} + K_{a1}K_{a2}}\right\} b[Fe^{III}\text{porphyrin}]_{total} \quad (3)$$

various porphyrin species ($\mathbf{p}H_2$, $\mathbf{p}H$, and $\mathbf{p}$, defined in eqs 4a and 4b), K_{a1} and K_{a2} are the acid dissociation constants (see eqs 4a and 4b), b is the pathlength of the cell, and $[Fe^{III}\text{-porphyrin}]_{total}$ is the sum of the concentrations of all porphyrin species. The first inflection in the plots of Figure 4 between pH 5 and 6 corresponds to pK_{a1} of the dihydrate $(\mathbf{3})Fe^{III}(H_2O)_2$ (eq 4a). The second inflection (pH ~9.5) at 417 nm is due to the second acid dissociation of $(\mathbf{3})Fe^{III}(H_2O)(OH)$ (eq 4b).

$$\underset{(\mathbf{p}H_2)}{(\mathbf{3})Fe^{III}(H_2O)_2} \xrightarrow[+H^+]{\overset{K_{a1}}{-H^+}} \underset{(\mathbf{p}H)}{(\mathbf{3})Fe^{III}(H_2O)(OH)} \quad (4a)$$

$$\underset{(\mathbf{p}H)}{(\mathbf{3})Fe^{III}(H_2O)(OH)} \xrightarrow[+H^+]{\overset{K_{a2}}{-H^+}} \underset{(\mathbf{p})}{(\mathbf{3})Fe^{III}(OH)_2} \quad (4b)$$

Spectrophotometric determinations of pK_{a1}' and pK_{a2}' were performed at various ionic strengths (maintained with $NaNO_3$),

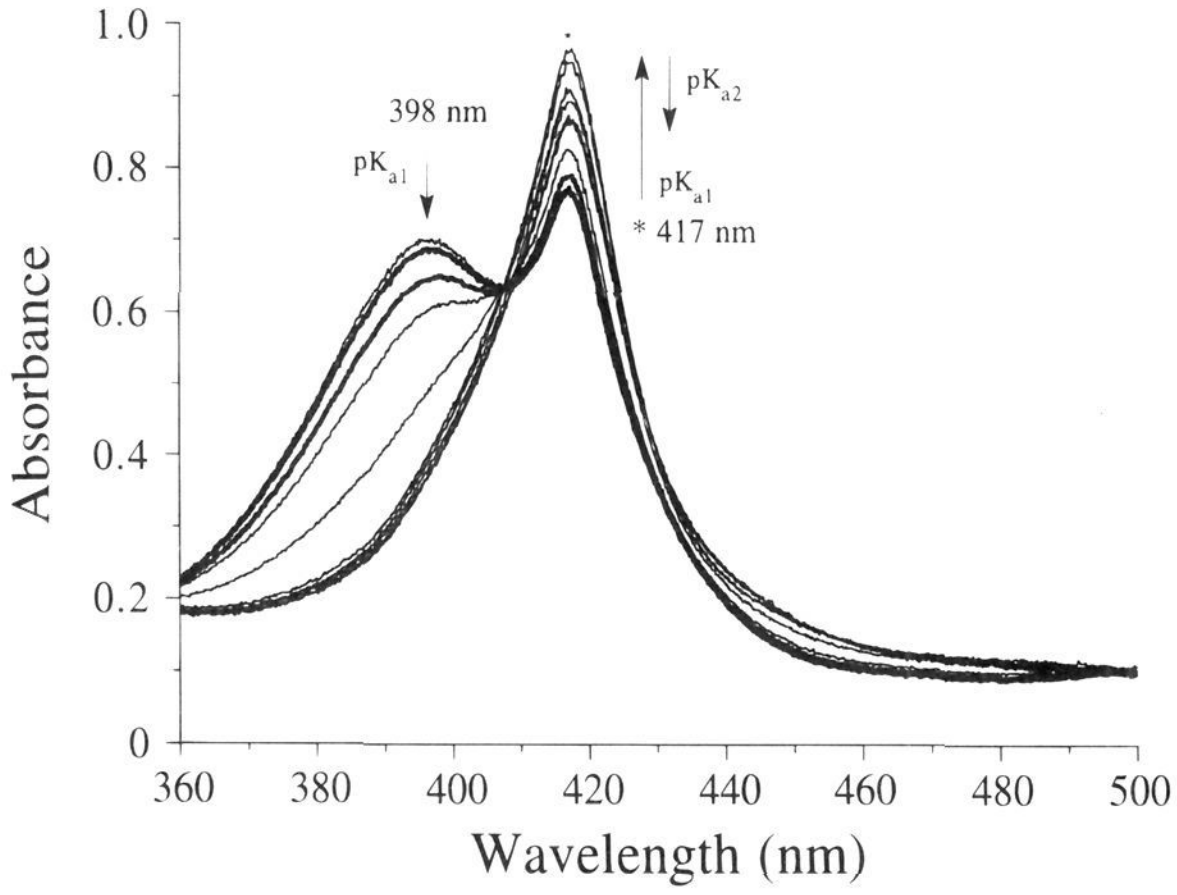

Figure 3. Visible absorption spectra for $(\mathbf{3})Fe^{III}(X)_2$ as a function of pH. A titration was performed at a fixed ionic strength of 0.2 by adding NaOH aliquots into a 25.0 mL cuvette (pathlength 3.387 cm).

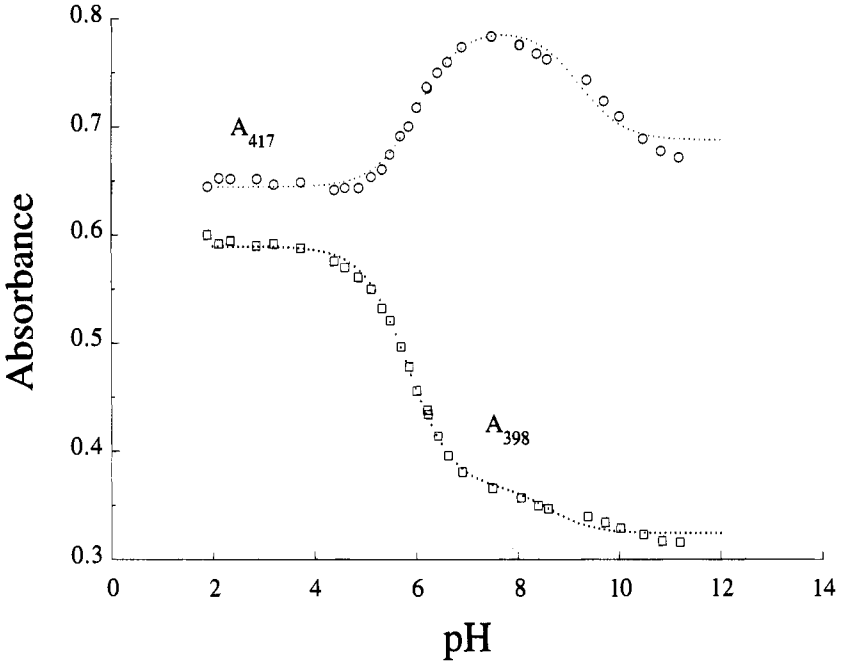

Figure 4. Plot of visible absorbance changes for (**3**)$Fe^{III}(X)_2$ as a function of pH at 398 (squares) and 417 nm (circles). The lines are theoretical fits to an equation of two consecutive acid dissociations (eq 3).

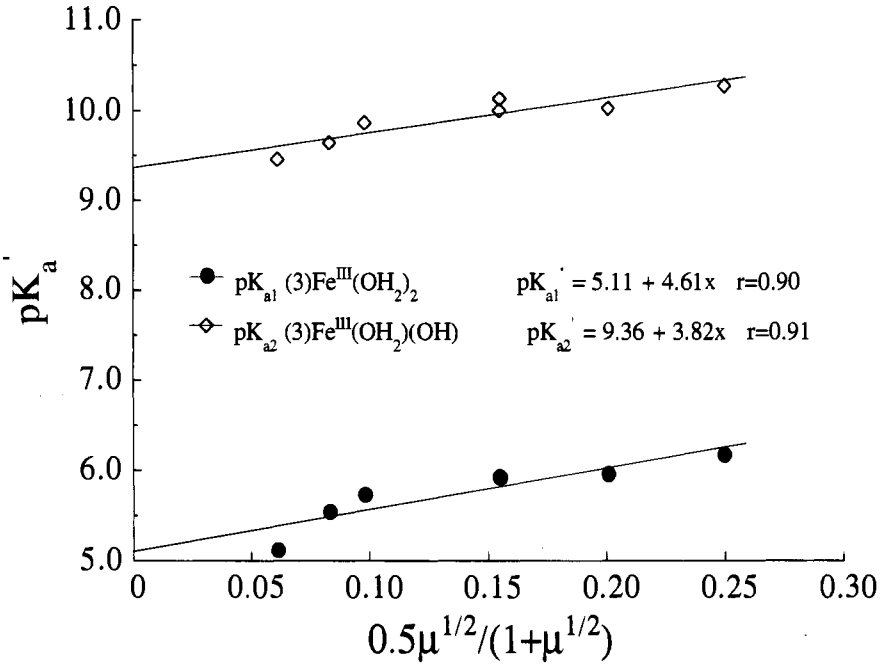

Figure 5. Plots of observed values of pK_{a1} (circles) for (**3**)$Fe^{III}(H_2O)_2$ (pK_{a1} at zero ionic strength = 5.11), pK_{a2} (diamonds) for (**3**)$Fe^{III}(H_2O)(OH)$ (pK_{a2} at zero ionic strength = 9.36), and pK_a (crosses) for (**1**)$Fe^{III}(H_2O)_2$ (pK_a at zero ionic strength = 7.24), as a function of $0.5\mu^{1/2}/(1+\mu^{1/2})$. For structures, see Charts 1 and 2 and the text. The ionic strength μ was maintained with $NaNO_3$ and titrations were performed over a range of μ from 0.05−1.0.

and the data fit, as before, to a standard expression for two consecutive acid dissociations (eq 3). Values of pK_{a1}' and pK_{a2}' obtained from fitting the data at 417 nm were found to increase with increased ionic strength. Equation 5 is the Güntelberg

$$pK_a' = pK_a + (Z_{HB}^2 - Z_B^2)\left[\frac{0.5\mu^{1/2}}{(1+\mu^{1/2})}\right] \quad (5)$$

modification of the Debye−Hückel equation for single ion activities.[20] According to this relationship, a plot of pK_a vs $0.5\mu^{1/2}/(1+\mu^{1/2})$ should provide a straight line with a y-intercept corresponding to the pK_a at zero ionic strength. Figure 5 shows a plot of pK_{a1}' for (**3**)$Fe^{III}(H_2O)_2$ and pK_{a2}' of (**3**)$Fe^{III}(H_2O)$-(OH) vs $0.5\mu^{1/2}/(1+\mu^{1/2})$. The pK_{a1} and pK_{a2} at $\mu = 0.2$ (ionic strength employed in the kinetic studies of the following manuscript in this issue) are interpolated to be 5.8 and 10.0, respectively. The slopes of the lines for the cationic porphyrin (**3**)$Fe^{III}(H_2O)_2$ are positive, whereas the slope for the plot of pK_{a1}' vs $0.5\mu^{1/2}/(1+\mu^{1/2})$ for the anionic (**1**)$Fe^{III}(H_2O)_2$ is negative.

(19) AT Biochem 1993, 20% commercial solution with a fixed cross-linking is diluted appropriately with electrophoresis buffer. *Note: Solutions of hydrolink D-600 should be treated with the same caution as polyacrylamide gel solutions.*

(20) *Aquatic Chemistry*; Stumm, W.; Morgan, J. J., Eds.; Wiley: New York, 1981; p 136.

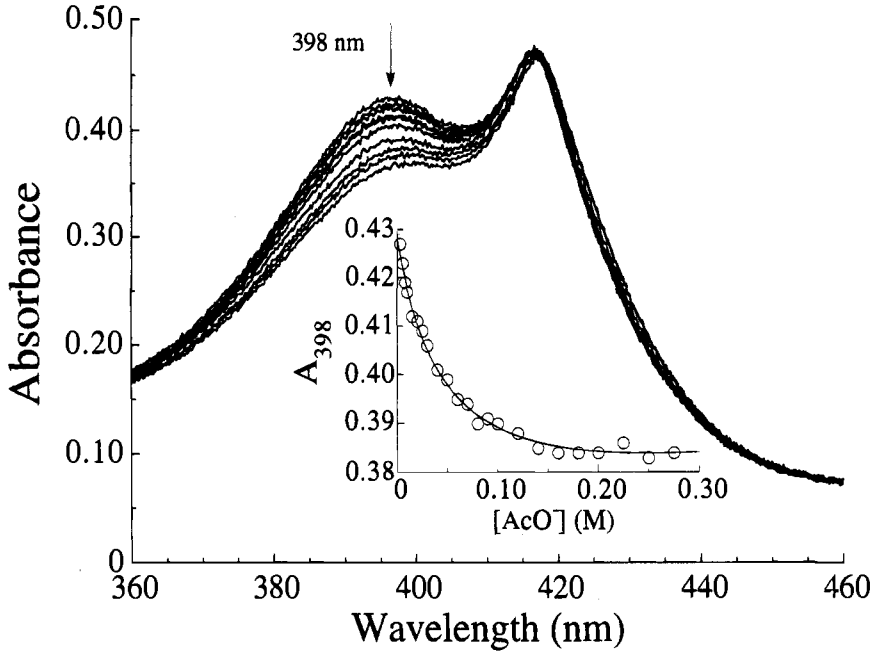

Figure 6. Visible absorption spectra for (**3**)$Fe^{III}(X)_2$ as a function of total acetate buffer concentration at pH 4.7. A titration was performed by addition of 4.4 M acetate stock solution at pH 4.70 into a 25.0 mL cuvette (pathlength 3.387 cm). Inset: Plot of absorbance changes at 398 nm for (**3**)$Fe^{III}(X)_2$ as a function of total acetate buffer concentration at pH 4.7. A pH-independent association constant for monoligation of acetate anion to (**3**)$Fe^{III}(X)_2$ (K_B) was calculated as 35 M^{-1} from fitting of the data to eq 8 (dotted line). The pH-independent value of K_B, averaged from titration experiments at pH 4.7 and pH 5.5, was calculated to be 42 ± 7 M^{-1}.

Equilibrium Complexation of Carboxyl Anions with the Iron of {(3)Fe^{III}}$^{9+}$. Weakly basic anions, such as carboxylates, are capable of complexing the metal ion of (**3**)$Fe^{III}(H_2O)_2$ by displacement of a water molecule. Equations 6a–c give the pertinent equilibria which affect the ligation of acetate anion (AcO^-) to (**3**)$Fe^{III}(H_2O)_2$. In our treatment, we assume (i) that only (**3**)$Fe^{III}(H_2O)_2$ ligates anions (eq 6c) and (ii) that (**3**)$Fe^{III}(H_2O)(OH)$ does

$$(\mathbf{3})Fe^{III}(H_2O)_2 \underset{+H^+}{\overset{K_1}{\underset{-H^+}{\rightleftharpoons}}} (\mathbf{3})Fe^{III}(H_2O)(OH) \qquad (6a)$$

$$HOAc \underset{+H^+}{\overset{K_a}{\underset{-H^+}{\rightleftharpoons}}} AcO^- \qquad (6b)$$

$$(\mathbf{3})Fe^{III}(H_2O)_2 \underset{-AcO^-}{\overset{K_B}{\underset{+AcO^-}{\rightleftharpoons}}} (\mathbf{3})Fe^{III}(H_2O)(OAc) \qquad (6c)$$

not absorb significantly compared with (**3**)$Fe^{III}(H_2O)_2$ and (**3**)$Fe^{III}(H_2O)(OAc)$ in the visible spectra in the region of 398 nm. The higher affinity of (**3**)$Fe^{III}(H_2O)_2$ for anions compared with (**3**)$Fe^{III}(H_2O)(OH)$ {assumption (i)} is rationalized by the fact that the former requires an anion to cancel the net +1 charge at the iron center. Assumption (ii) is justified, since the (**3**)$Fe^{III}(H_2O)(OH)$ form has a much smaller extinction coefficient at 398 nm, compared with (**3**)$Fe^{III}(H_2O)_2$ (see Figure 3) and (**3**)$Fe^{III}(H_2O)(OAc)$ (Figure 6). Hence, the total absorbance at 398 nm is the sum of the contributions of (**3**)$Fe^{III}(H_2O)_2$ and the acetate ligated form (**3**)$Fe^{III}(H_2O)(OAc)$ (eq 7). Equation 7 as well as the appropriate expression of mass balance

$$A_{398} = b\{\epsilon_0[(\mathbf{3})Fe^{III}(H_2O)_2] + \epsilon_B[(\mathbf{3})Fe^{III}(H_2O)(OAc)]\} \quad (7)$$

$\{[(\mathbf{3})Fe^{III}]_{total} = [(\mathbf{3})Fe^{III}(H_2O)_2] + [(\mathbf{3})Fe^{III}(H_2O)(OH)] + [(\mathbf{3})Fe^{III}(H_2O)(OAc)]\}$ and expressions involving the equilibrium constants in eqs 6a–c were used to derive eq 8, where the total absorbance at 398 nm is shown as a function of total acetate buffer concentration ($[HOAc]_t = [HOAc] + [AcO^-]$). In eq 8, $[P]_t$ is the total concentration of all porphyrin species,

$$A_{398} = [P]_t b \frac{a_H\left\{\epsilon_0 + \dfrac{\epsilon_B K_a K_B [HOAc]_t}{(K_a + a_H)}\right\}}{\left\{(K_1 + a_H) + \dfrac{a_H K_a K_B [HOAc]_t}{(K_a + a_H)}\right\}} \qquad (8)$$

b is the pathlength of the cuvette (3.387 cm), ϵ_o and ϵ_B are the extinction coefficients of (**3**)$Fe^{III}(H_2O)_2$ and (**3**)$Fe^{III}(H_2O)(OAc)$ at 398 nm, respectively, a_H is the hydrogen ion activity, K_a is the acid dissociation constant of acetic acid in water at 30 °C, K_1 is the apparent acid dissociation constant of (**3**)$Fe^{III}(H_2O)_2$, and K_B is the pH-independent acetate ligation constant. Figure 6 shows absorption spectra at various total concentrations of acetate buffer, obtained from a titration of (**3**)$Fe^{III}(H_2O)_2$ with 4.4 M $[HOAc]_t$ at pH 4.7. In the inset to Figure 6, the absorbances at 398 nm are plotted as a function of $[HOAc]_t$, and the line which fits the experimental points was generated by use of eq 8. The pH-independent value for K_B, obtained by averaging the K_B values from fitting of the data from experiments at pH 4.7 and 5.5, is 42 ± 7 M^{-1}. The values for extinction coefficient of (**3**)$Fe^{III}(H_2O)(OAc)$ {ϵ_B} used in generating the fit in Figure 6 were relatively unaltered by the pH of the titration experiment {2.2 × 10^5 and 2.3 × 10^5 at pH 4.7 and 5.5, respectively}, while those calculated for (**3**)$Fe^{III}(H_2O)_2$ {ϵ_o} were 2.7 × 10^5 and 3.7 × 10^5 at pH 4.7 and 5.5, respectively. By the known dependence of K_1 of (**3**)$Fe^{III}(H_2O)_2$ upon the ionic strength of the solution (Figure 5) the values of K_1 employed in the generation of the fits correspond to an ionic strength of 0.2 (pH 4.7) and 0.4 (pH 5.5). It was not possible to maintain constant ionic strength in the course of the titrations. It is reasonable to expect, however, that the ionic strength is higher in the experiment at the higher pH, where both acids {HOAc and (**3**)$Fe^{III}(H_2O)_2$} are dissociated to a greater extent.

Discussion

A new polycationic, water soluble porphyrin ligand $3H_2$ has been synthesized and characterized. The synthesis of $3H_2$ and its iron(III) complex (**3**)$Fe^{III}(X)_2$ (Chart 1 and Figure 1) is given in Scheme 2. The success of the procedure rests on the discovery of a highly efficient and selective bromomethylation of tetramesitylporphyrin {$TMPH_2$}, a commonly known and readily available porphyrin. $TMPH_2$ reacts with paraformaldehyde in HBr/HOAc to give ultimately the octakis(bromomethyl) derivative **4**. In the highly acidic reaction mixture, the deep green color indicates that the porphyrin intermediates are present in diprotonated form. Porphyrin protonation renders the β-pyrrole positions of the ring unreactive to electrophilic aromatic substitutions. Therefore, only the unsubstituted meta positions on the *meso*-phenyl rings of $TMPH_2$ and intermediates **5a**−**g** in Table 1 are found to be reactive. $3H_2$ and (**3**)$Fe^{III}(X)_2$ are synthesized by simple bromide displacement by trimethylamine, followed by insertion of Fe(II) in air in refluxing aqueous solution, respectively. Purification of the cationic compounds is achieved by combinations of gel filtration, anion exchange chromatography, and membrane ultrafiltration.

Porphyrin $3H_2$ was characterized by ^1H and ^{13}C NMR, UV−visible spectroscopy, and gel electrophoresis (Figure 2). (**3**)$Fe^{III}(X)_2$ was judged pure by UV−visible spectra (by the absence of free base porphyrin and ferrous ion) and by gel electrophoresis. The application of gel electrophoretic separation for the identification of charged water soluble porphyrins has a recent precedent[21] and shows promise as a useful technique for analysis of these types of compounds. In particular, the use of hydrolink D-600 as the gel material vs high density polyacrylamide or agarose gels[21] seems to offer the advantage of allowing separation of free base porphyrins and their metalated counterparts (Figure 2). The technique demonstrates the strict monomeric nature of (**3**)$Fe^{III}(X)_2$. In contrast to commercially available (**TMAP**)$Fe^{III}(X)_2$ and (**TMPyP**)$Fe^{III}(X)_2$ (Chart 2), which form μ-oxo dimers on the gel (Figure 2), no extra fast migrating bands for (**3**)$Fe^{III}(X)_2$ can be detected. (**3**)$Fe^{III}(X)_2$ therefore fulfills our stated requirements, being polycationic in nature, but sufficiently hindered to prevent unwanted dimerization and aggregation. A model of (**3**)$Fe^{III}(H_2O)_2$ (Figure 1) places the nitrogens of the $-NMe_3^+$ groups at an average of 8.4 Å distance from the axially ligated water molecule closest (on the same face of the porphyrin). (**1**)$Fe^{III}(H_2O)_2$ (Chart 1) places the oxygens of $-SO_3^-$ groups at a minimum of 7.3 Å from the closest ligated water molecule. These structural features of (**1**)$Fe^{III}(H_2O)_2$ and (**3**)$Fe^{III}(H_2O)_2$ are central to our discussion of peripheral electronic factors.

Spectrophotometric pK_a determinations demonstrated the influence of charge effects on the acid dissociation constants of the water molecules ligated to the metal of (**3**)$Fe^{III}(H_2O)_2$. Plots of apparent first pK_a values (pK_{a1}') of ligated water (as in eq 4a) vs $0.5\mu^{1/2}/(1+\mu^{1/2})$ for the charged iron(III) porphyrins (**1**)$Fe^{III}(H_2O)_2$ and (**3**)$Fe^{III}(H_2O)_2$ demonstrate the effect of overall molecular charge on the ionic strength dependence of pK_a (Figure 5). The lowering of pK_a values for (**3**)$Fe^{III}(H_2O)_2$ compared with (**1**)$Fe^{III}(H_2O)_2$ is due to the cationic environment surrounding the water molecules in the former. The behavior of (**3**)$Fe^{III}(H_2O)_2$ parallels the observed dependence of pK_a' on μ for the tetracationic ($\alpha\beta\alpha\beta$-**TMNP**)$Fe^{III}(H_2O)_2$, studied by Miskelly et al.[12] Inspection of the X-ray crystal structure of the related {($\alpha\alpha\alpha\alpha$-**TMNP**)Fe^{III}}[22] (Cambridge Structural Database file CEXGIV) and a molecular model of ($\alpha\beta\alpha\beta$-**TMNP**)$Fe^{III}(H_2O)_2$, based on the aforementioned crystal structure, indicates that the ligated water on iron is ~5 Å from the nitrogen atom N1 of the nicotinamide ring (naively assumed to be the center of the positive charge). Molecular models of (**3**)$Fe^{III}(H_2O)_2$ (Figure 1) and (**1**)$Fe^{III}(H_2O)_2$ have water oxygens 8.4 and 7.3 Å away from the "centers of charge" {$>N<^+$ and $(-SO_2)O^-$, respectively}. The slopes of the plots of pK_a' vs $0.5\mu^{1/2}/(1+\mu^{1/2})$ are of approximately equal value but opposite sign for (**3**)$Fe^{III}(H_2O)_2$ and (**1**)$Fe^{III}(H_2O)_2$, respectively. Therefore, at the ionic strengths employed, two cationic charges belonging to $-NMe_3^+$ substituents provide the same alteration of pK_a, of opposite sign, as one $-SO_3^-$ group at approximately the same distance.

The cationic charges arrayed on the porphyrin ring around the iron(III) of (**3**)$Fe^{III}(H_2O)_2$ cause oxyanions to displace H_2O and ligate to the iron atom. This contrasts the behavior of (**1**)$Fe^{III}(H_2O)_2$ and (**2**)$Fe^{III}(H_2O)_2$, which do not appear to measurably ligate weakly basic anions. As an example, the weak base acetate complexes the iron(III) of (**3**)$Fe^{III}(H_2O)_2$ (Figure 6 and eq 6c). The pH-independent association constant K_B for monoligation of acetate to (**3**)$Fe^{III}(H_2O)_2$ (eq 6c) is 42 ± 7 M^{-1}. The favored monoligation by the weak base AcO^- to (**3**)$Fe^{III}(H_2O)_2$ results in cancellation of the net +1 charge at the iron(III) center.

In conclusion, a new polycationic porphyrin ligand $3H_2$ and iron(III) complex are reported. (**3**)$Fe^{III}(X)_2$, a dihydrated iron(III) porphyrin, is monomeric in aqueous solution at all pH values and concentrations employed. The mechanisms of reactions of hydroperoxides with (**3**)$Fe^{III}(X)_2$ is the subject of our current efforts (see the following paper in this issue).

Acknowledgment. Ö.A. thanks the American-Scandinavian Foundation for partial financial support in the form of fellowships. This study was supported by the National Institutes of Health.

JA9416293

(21) Buchler, J. W.; Künzel, F. M.; Mayer, U.; Nawra, M. *Fresenius J. Anal. Chem.* **1994**, *348*, 371.

(22) Gunter, M. J.; McLaughlin, G. M.; Berry, K. J.; Murray, K. S.; Irving, M.; Clark, P. E. *Inorg. Chem.* **1984**, *23*, 283.